Preparation of polyaniline–Fe$_2$O$_3$ composite and its anticorrosion performance

S. Sathiyanarayanan, S. Syed Azim, G. Venkatachari [*]

Central Electrochemical Research Institute, Karaikudi 630006, India

Abstract

Polyaniline–Fe$_2$O$_3$ composites were chemically prepared by oxidative polymerization of aniline in phosphoric acid medium with ammonium persulphate as oxidant. Different ratios of aniline–Fe$_2$O$_3$ were taken to prepare polyaniline–Fe$_2$O$_3$ composites, i.e. 1:2, 1:1, 2:1. The composites were characterized by FTIR, XRD and SEM. Using the prepared composites, primer paints with acrylic binder were prepared and coated on the steel samples. The corrosion protection ability of the coating was found out by EIS method in 3% NaCl solution. It has been found that the coating with composite of 1:1 ratio of aniline:Fe$_2$O$_3$ is found to offer higher protection than the coating with other ratios and plain Fe$_2$O$_3$.
© 2007 Elsevier B.V. All rights reserved.

Keywords: Polyaniline; Polyaniline–Fe$_2$O$_3$ composite; EIS; FTIR; Corrosion protection; Steel

1. Introduction

Organic coatings are widely used for corrosion protection of metals. Most of the primer coatings contain iron oxide (Fe$_2$O$_3$) as one of the pigment. Several studies [1–26] have shown that polyaniline containing organic coatings offer efficient corrosion protection of steel. Coatings containing polyaniline have been shown to protect steel at pinhole and scratches [9,12]. It has been reported that polyaniline containing coatings protect steel by forming a passive layer on the iron surface [5,16,21]. Hence, it is envisaged that polyaniline-coated iron oxide containing coatings can exhibit better corrosion protection ability of iron. Earlier studies on polyaniline–Fe$_2$O$_3$ composites were mostly concerned with their conductivity and magnetic properties [27,28]. Therefore, PANI coated Fe$_2$O$_3$ composites were prepared by in situ polymerization and examined their corrosion protection performance of steel. The results of the study are presented in this paper.

2. Experimental

2.1. Materials

Aniline (A.R.) and ammonium persulphate (A.R.) both were obtained from Sd-Fine Chemicals (India). The monomer was distilled over zinc dust and was kept in dark prior to use. The commercially available iron oxide pigment with particle size of 2–3 μm was used.

2.2. Preparation of PANI–Fe$_2$O$_3$ composites

One molar of distilled aniline was dissolved in 500 ml of 1M solution of phosphoric acid and the required quantity of Fe$_2$O$_3$ was added to it. The mixture was stirred well. Pre-cooled 500 ml of 1M solution of ammonium persulfate was added drop wise to the pre-cooled aniline–acid–Fe$_2$O$_3$ mixture for about 1.5 h with constant stirring. The reaction was conducted at 5 ± 1 °C. After the addition, the stirring was continued for 2 h for ensuring complete polymerization. A dark green coloured PANI–Fe$_2$O$_3$ composite thus formed was filtered and repeatedly washed with distilled water to remove excess acid content. The polymer composite was dried in oven at about 80 °C for 2 h. The polymer composites of different ratios of aniline:Fe$_2$O$_3$, i.e. 1:2, 1:1 and

---
[*] Corresponding author.
E-mail address: gvchari@gmail.com (G. Venkatachari).

2:1 were prepared. The dried PANI–Fe_2O_3 composite (PFC) was fine grinded using morter and then used as pigment.

The point of zero charge of Fe_2O_3 is reported to be around 7.2 [29,30]. Hence, it may be positively charged in the H_3PO_4 bath. Due to this, the $H_2PO_4^-$ ions adsorb on Fe_2O_3 and this adsorbed ions can work as charge compensator for positively charged PANI chain in the formation of polyaniline–Fe_2O_3 composite. Similar mechanism has been reported for the synthesis of PANI–MnO_2 composite [31].

2.3. Characterization of PANI–Fe₂O₃ composites (PFC)

The infrared spectra of the polymer composite were recorded on NICOLET 380 FTIR spectrometer in KBr medium at room temperature in the region of 2000–500 cm^{-1}. X-ray diffraction pattern of PANI–Fe_2O_3 composites were taken with Analytical (Model PW3040/60) X-ray diffractometer using Cu Kα radiation in the 2θ range 0–90° at the scan range of 0.0170° 2θ with continuous scan type with scan step time of 15.5056 s. The morphology of the composites was analyzed using Hitachi (Model S3000 H) scanning electron microscopy by spreading the composite over a copper block over which gold was sputtered. The electrical conductivity of the composite was found by four probe resistivity meter.

2.4. Preparation of PANI–Fe₂O₃ composite (PFC) containing paint

The primer is formulated using commercial acrylic resin (Kondicryl 166, Pidilite, India). The volume solids of the formulation was kept at 30% with 35% pigment volume concentration (P.V.C.). The main pigments used in this formulation were polyaniline, titanium-di-oxide and PFC along with mica and silica as extender pigments. Di-octyl-phosphate (D.O.P.) was used as a plasticizer.

The pigments were pre-mixed and the paint was prepared in a lab attritor. The attritor was run for 45–50 min. The fineness of dispersion of paint was found using Hegmann gauge and it was found to be between 7 and 8. The paint was stored in an air tight container. The specific gravity of the paint was 1.0. The dry film thickness (DFT) of the coating was measured by Minitest thickness meter (Model 600, Electrophysick). The adhesion of the coating was tested by Tape test as per ASTM D3359-02 and found to pass the test.

2.5. Evaluation of corrosion resistant properties of the coating by EIS studies

Steel specimens of size 5 cm × 5 cm × 0.1 cm were sandblasted (SA 2.5) and degreased with trichloroethylene and coated with the developed paint. The total thickness of the coating was 40 ± 2 μm. A glass tube of 1.2 cm diameter of length 3 cm was fixed on the coated steel with adhesive (m seal) and the exposed area was 1.0 cm^2 to the solution. The solution of 3% NaCl was taken in the glass tube. A platinum foil and a saturated calomel electrode were placed inside the glass tube. The schematic diagram of the experimental cell
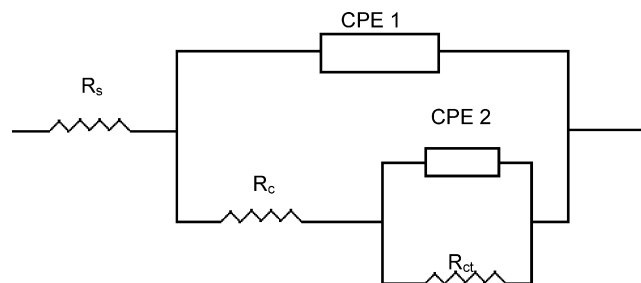

Fig. 1. Equivalent circuit of painted panel.

assembly is described elsewhere [32]. The assembly was connected to electrochemical impedance analyzer (PARSTAT 2273, EG&G). Impedance measurements were carried out for a frequency range of 100 KHz to 0.01 Hz with an ac amplitude of 20 mV for different immersion time up to 5 days using POWER SINE software. The impedance values are reproducible ±2 to 3%. From the impedance plots, the coating resistance (R_c), the coating capacitance (C_c), the charge transfer resistance (R_{ct}) and the double layer capacitance (C_{dl}) values were calculated using the equivalent circuit shown in Fig. 1. In the equivalent circuit, R_s represents the solution resistance, R_c represents the coating resistance, CPE 1 represents the constant phase element for coating capacitance, R_{ct} represents the charge transfer resistance and CPE 2 represents the constant phase element for double layer capacitance.

For the description of a frequency independent phase shift between an applied AC potential and its current response, a constant phase element (CPE) is used which is defined in impedance representation as

$$Z(CPE) = Y_0^{-1}(j\omega)^{-n}$$

where Y_0 is the CPE constant, ω the angular frequency (in rad s^{-1}), $j^2 = -1$ the imaginary number and n is the CPE exponent. Depending on n, CPE can represent resistance ($Z(CPE) = R$, $n = 0$), capacitance ($Z(CPE) = C$, $n = 1$), inductance ($Z(CPE) = L$, $n = -1$) or Warburg impedance for ($n = 0.5$) [33]. The following equations have been used to convert Y_0 into coating capacitance C_c and double layer capacitance C_{dl} [34] from the impedance values of high and low frequency semicircles,

$$C_c \text{ or } C_{dl} = y_0(\omega_m'')^{n-1}$$

where ω_m'' is the angular frequency at which Z'' is maxiumum of the corresponding semicircle.

3. Results and discussion

3.1. FTIR spectral characterization

Fig. 2(A) shows the FTIR spectra of Fe_2O_3 and PANI. The bands at 1561 and 1474 cm^{-1} of PANI (curve a) are the stretching mode of C=N and C=C of quinoid and benzenoid rings. The bands at 1296 and 1242 cm^{-1} have been attributed to C–N stretching mode of benzenoid ring and band at 1110 cm^{-1} is due to a plane bending vibration of C–H. The curve b in Fig. 2(A)
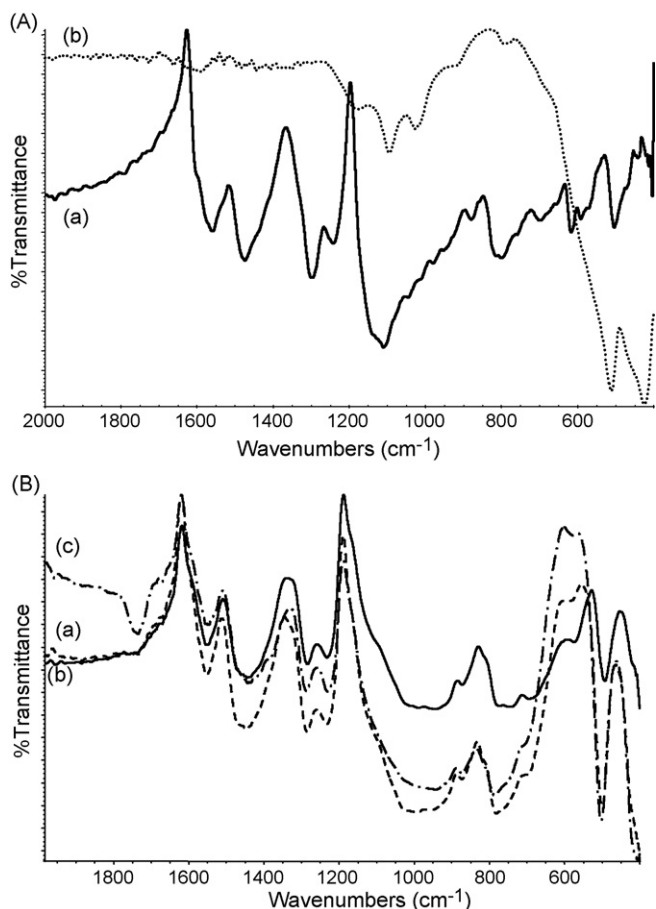
Fig. 2. (A) FTIR spectra of PANI and Fe_2O_3: (a) PANI; (b) Fe_2O_3. (B) FTIR spectra of PANI–Fe_2O_3 composites: (a) 1:1 composite; (b) 1:2 composite; (c) 2:1 composite.

indicates the FTIR spectra of Fe_2O_3, where the bands around 500–400 cm^{-1} are assigned to Fe–O stretch. The FTIR spectra of PFC are shown in Fig. 2(B). It can be seen that the FTIR spectra of the composites are similar to that of pure PANI while the bands for C=N, C=C and C–N all shifted to lower wave numbers, i.e. 1555, 1444, 1285 and 1233 cm^{-1} due to strong interaction of Fe_2O_3 and polyaniline. Such type of red shift has been reported for PANI–TiO_2 [35], PANI–Fe_3O_4 [27], PANI–MnO_2 [31] and PANI–ZrO_2 [36] composites.

3.2. XRD characterization

Fig. 3(a) shows the X-ray diffraction pattern of PANI. Diffraction pattern of PANI have a broad peak at about $2\theta = 25.0$ which is the characteristic peak of PANI [37,38]. Fig 3(b) shows the XRD pattern of Fe_2O_3 and Fig 3(c) shows the XRD pattern of PFC (1:1). It can be seen that the PFC XRD pattern is very much similar to that of Fe_2O_3 and the broad diffractive peak of PANI has become weak. This indicates that PANI deposited on the surface of Fe_2O_3 has no effect on the crystalline structure of Fe_2O_3. Besides, these results indicate that PANI is amorphous in the PANI–Fe_2O_3 composite since the molecular chain of the adsorbed PANI is confined and the degree of crystallinity is decreased [39].
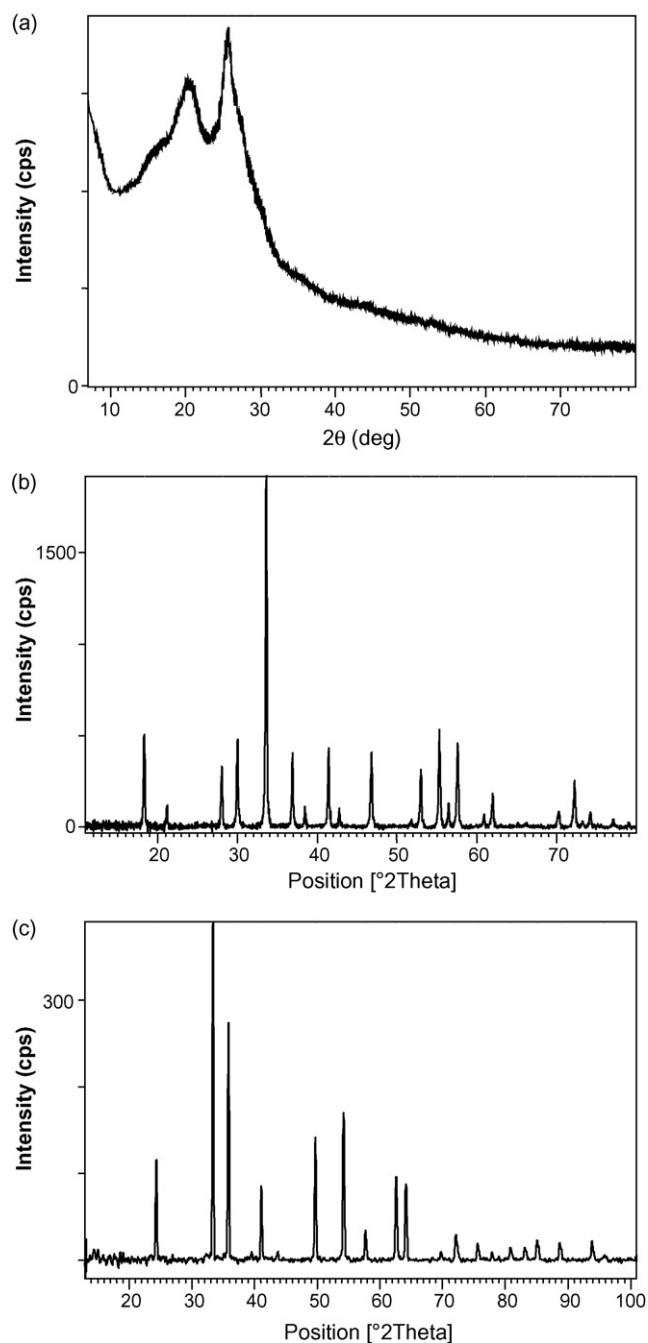

Fig. 3. XRD pattern of PANI and PFC: (a) PANI; (b) Fe_2O_3; (c) PFC (1:1).

3.3. Morphology of the composites

Fig. 4(a–e) shows the SEM pictures of Fe_2O_3, PANI and PFCs. Morphology examinations revealed that at higher ratios of Fe_2O_3:aniline, the round shaped Fe_2O_3 particles with few PANI adhered are observed due to preferential polymerization of aniline on Fe_2O_3 particles while at lower ratios, Fe_2O_3 particles with thick PANI layer and adsorbed PANI particles are observed due to secondary nucleation effect of primary formed PANI layer. Besides, the colour of the composites was found to be dark brown in the case of higher Fe_2O_3 content while the composite appeared dark green for lower Fe_2O_3 content. No
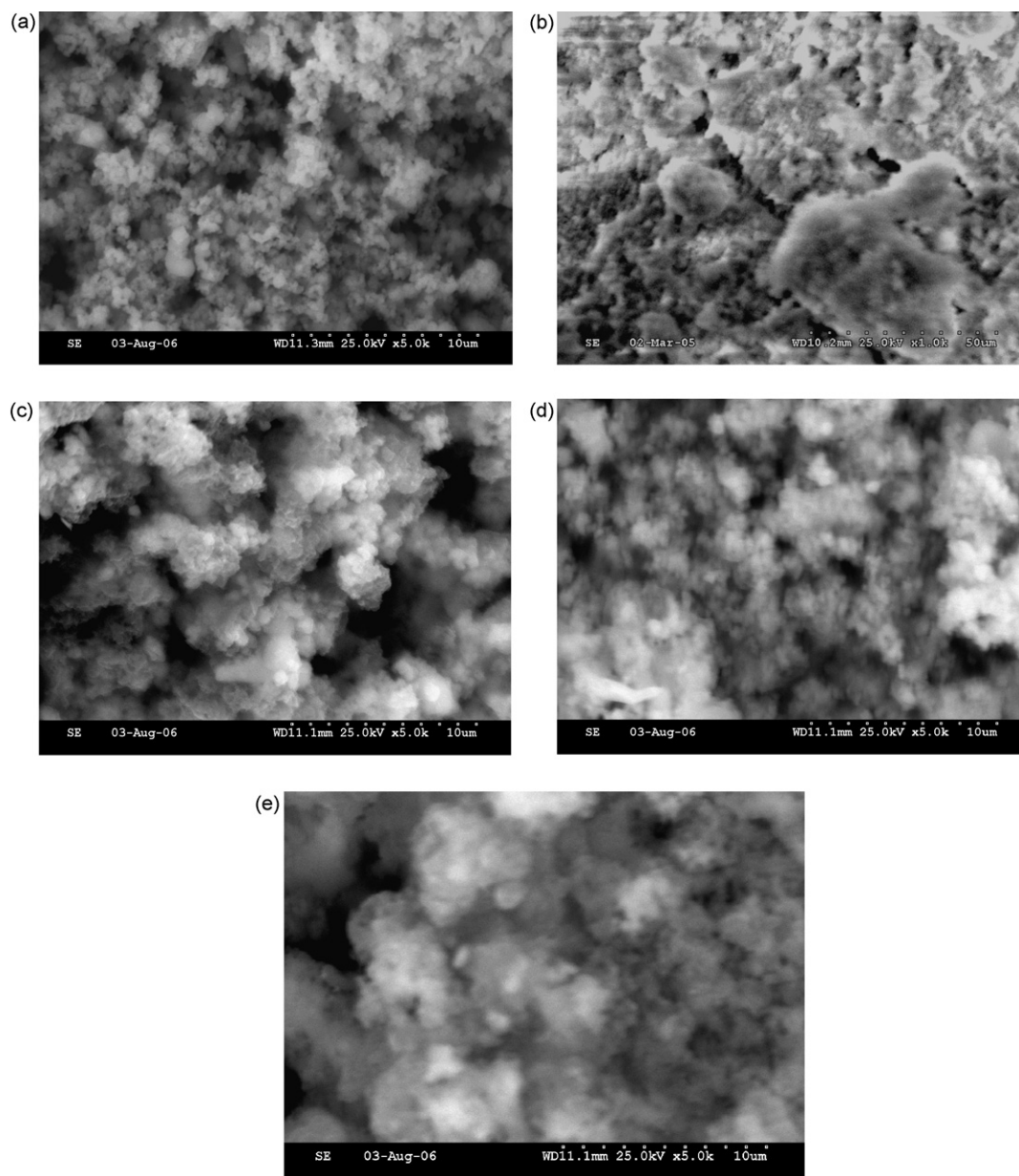
Fig. 4. SEM pictures of PANI and PFC: (a) Fe_2O_3; (b) PANI; (c) PFC (1:1); (d) PFC (1:2); (e) PFC (2:1).

peel off the PANI layers was observed for all samples indicated the good adhesion of the PANI layer on the Fe_2O_3 particles.

3.4. Conductivity characteristics

The conductivity values obtained for the pure PANI and PFC are PANI: 2.17 S cm^{-1}; PFC (1:2): 0.04 S cm^{-1}; PFC (1:1): 0.025 S cm^{-1} and PFC (2:1): 0.033 S cm^{-1}. It can be seen that the composites have the same order of conductivity. However, these values are two orders less than the conductivity of PANI.

3.5. EIS measurements

The corrosion protection performance of the coating containing Fe_2O_3, Fe_2O_3 + PANI and PFC have been found by

EIS method on the coated panels in 3% NaCl solution. Fig. 5 shows the impedance behaviour of Fe_2O_3 containing coating and Table 1 gives the impedance parameters derived from these curves. The resistance of the coating is found to be decreased from 74.7 to 5 kΩ cm^2 after 3 days immersion and attained 1.4 kΩ cm^2 after 5 days immersion. The R_{ct} values are also decreased from 45 to 1.5 kΩ cm^2 after 5 days immersion. This indicates the loss of protective property after 3 days of immersion. This observation has been confirmed by the marked increase of C_{dl} values from 1.5×10^{-8} to 5.2×10^{-3} F cm^{-2}.

Fig. 6 shows the impedance behaviour of coating containing Fe_2O_3 and PANI added separately in 3% NaCl. The impedance parameters obtained from these curves are also given in Table 1. The coating resistance which is 4.91 kΩ cm^2

Table 1
Impedance parameters of Fe_2O_3 and Fe_2O_3 + PANI pigmented coatings on steel in 3% NaCl

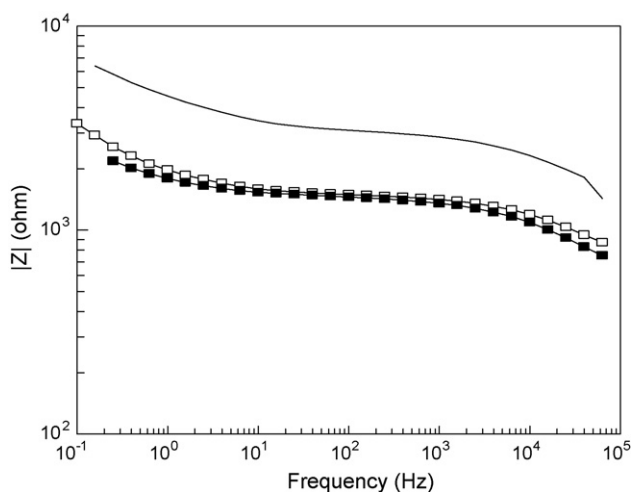| Time days	Coating resistance R_c (Ω cm^2)	Coating capacitance C_c (F cm^{-2})	Charge transfer resistance R_{ct} (Ω cm^2)	Double layer capacitance C_{dl} (F cm^{-2})
Fe_2O_3				
1	7.47×10^4	3.53×10^{-8}	4.54×10^4	1.55×10^{-8}
3	5.00×10^3	4.48×10^{-8}	2.81×10^3	1.91×10^{-5}
5	1.42×10^3	1.70×10^{-7}	1.50×10^3	5.21×10^{-3}
Fe_2O_3 + PANI				
1	4.91×10^3	2.23×10^{-9}	1.57×10^4	9.17×10^{-8}
3	3.21×10^3	2.58×10^{-9}	8.66×10^3	1.70×10^{-8}
5	4.12×10^3	3.19×10^{-9}	8.51×10^3	5.80×10^{-8}

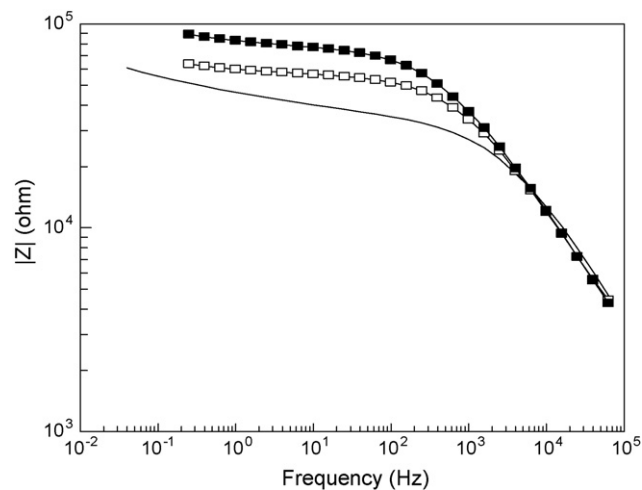Fig. 5. Impedance behaviour of Fe_2O_3 pigmented coating on steel in 3% NaCl. (–) 1 Day; (□) 3 days; (■) 5 days.

Fig. 7. Impedance behaviour of PFC (1:1) pigmented coating on steel in 3% NaCl. (–) 1 Day; (□) 3 days; (■) 5 days.

on 1st day drops to 4.12 kΩ cm^2 in 5 days. Similarly the charge transfer resistance R_{ct} is also decreased from 15.7 to 8.51 kΩ cm^2.

Figs. 7–9 show the variation of impedance of coating containing PFC with different ratios. Table 2 compares the variation of impedance values for coatings of different composites with

period of immersion. The resistance value of the coating for 1:1 composite is found to increase from 31.4 to 80.8 kΩ cm^2 with time and the R_{ct} values are remained in the range of 26.5–28.4 kΩ cm^2 with time. This indicates that the 1:1 composite is able to protect steel more effectively than the coating containing Fe_2O_3.
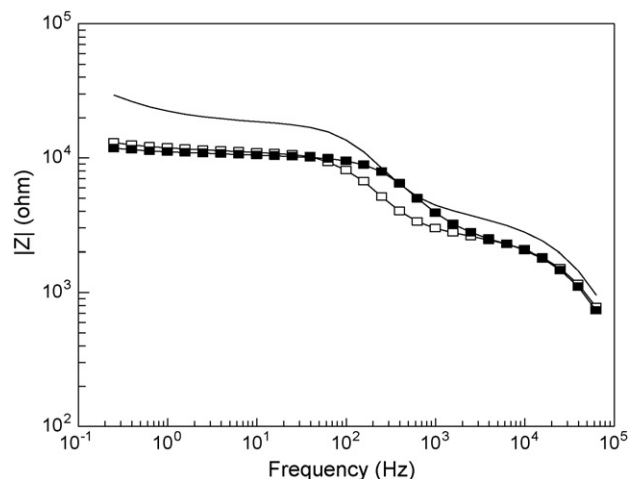

Fig. 6. Impedance behaviour of Fe_2O_3 + PANI pigmented coating on steel in 3% NaCl. (–) 1 Day; (□) 3 days; (■) 5 days.
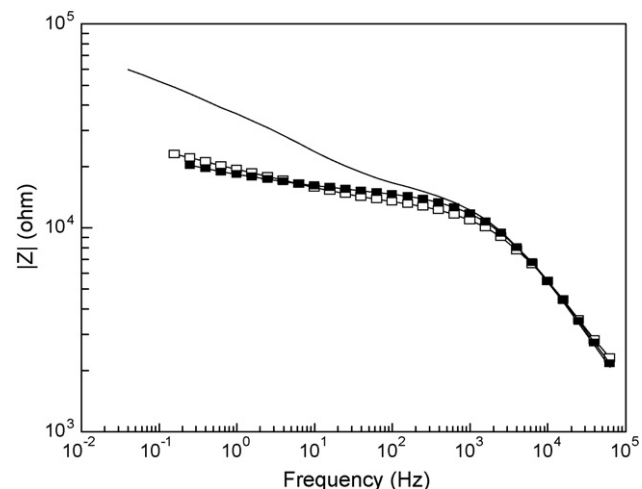

Fig. 8. Impedance behaviour of PFC (1:2) pigmented coating on steel in 3% NaCl. (–) 1 Day; (□) 3 days; (■) 5 days.

Table 2
Impedance parameters of PFC pigmented coatings on steel in 3% NaCl

| Time days	Coating resistance R_c ($\Omega\,cm^2$)	Coating capacitance C_c ($F\,cm^{-2}$)	Charge transfer resistance R_{ct} ($\Omega\,cm^2$)	Double layer capacitance C_{dl} ($F\,cm^{-2}$)
PFC (1:1)				
1	3.14×10^4	7.98×10^{-11}	2.65×10^4	1.88×10^{-10}
3	6.06×10^4	2.58×10^{-9}	2.60×10^4	5.12×10^{-10}
5	8.08×10^4	3.49×10^{-9}	2.84×10^4	5.26×10^{-8}
PFC (1:2)				
1	1.50×10^4	3.21×10^{-9}	6.21×10^4	1.11×10^{-5}
3	1.08×10^4	1.99×10^{-9}	4.98×10^4	2.36×10^{-3}
5	1.48×10^4	3.11×10^{-9}	1.21×10^4	1.53×10^{-3}
PFC (2:1)				
1	1.67×10^4	1.18×10^{-10}	4.23×10^4	3.33×10^{-10}
3	7.78×10^3	1.59×10^{-9}	6.00×10^3	1.16×10^{-5}
5	5.92×10^3	2.16×10^{-9}	4.00×10^3	1.21×10^{-3}
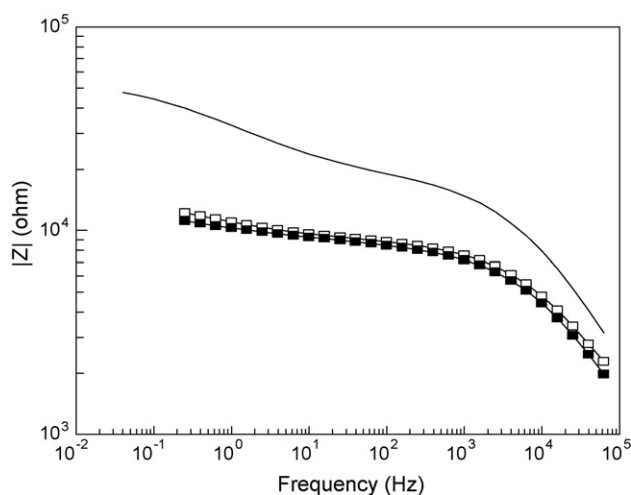
Fig. 9. Impedance behaviour of PFC (2:1) pigmented coating on steel in 3% NaCl. (–) 1 Day; (□) 3 days; (■) 5 days.

In the case of coating containing 1:2 composite, the coating resistance is found to be constant in the range of 15.0–14.8 k$\Omega\,cm^2$ with time. The charge transfer resistance values are decreased from 62.1 to 12.1 k$\Omega\,cm^2$ with time. Even though the coating capacitance values are remained at 3.2 to $3.1 \times 10^{-9}\,F\,cm^{-2}$ with time, the C_{dl} values are found to be very high, i.e. 1.11×10^{-5} to $1.5 \times 10^{-3}\,F\,cm^2$.

For the coating containing 2:1 composite there is a marked decrease of both coating resistance and charge transfer resistance values with time which indicates the poor protective property of the coating.

The above studies show that the coating containing PFC formed in 1:1 ratio is found to offer high corrosion protection than that of coating containing Fe_2O_3 and PFCs with 2:1 and 1:2 ratios. The corrosion protection ability of the PANI–Fe_2O_3 composite depends upon the morphology of PANI deposited on Fe_2O_3. In the case of 2:1 ratio (aniline:Fe_2O_3) even though the concentration of PANI deposit is more but the PANI deposits are granular due to secondary nucleation of PANI growth on the already existing PANI [40]. Similar observation has been reported in the case of preparation of PANI–SiO_2 composite [41] and PANI–zinc ferrite composite [42]. But in the case of 1:1 ratio, uniform, thin and adherent PANI coating is formed on Fe_2O_3. However, for 1:2 ratio, the Fe_2O_3 is not fully covered with polyaniline. Hence, the coating containing the PANI–Fe_2O_3 composite (1:1) is found to offer higher corrosion protection.

The better performance of the coating containing 1:1 composite may be due to uniform coverage of Fe_2O_3 by polyaniline polymer. It has been established in earlier studies [5,16,21] that the polyaniline containing coating is able to protect steel by passivation of iron substrate. From SEM and XPS studies, it has been reported that the oxide layer formed in PANI containing coating is mainly of Fe_2O_3 above a very thin Fe_3O_4 layer [16].

The corrosion protection of steel by PANI (ES) containing coating has been ascribed for substrate ennoblement, the formation of a passive oxide film and anodic inhibition through the precipitation of an insoluble metal salt and dopant anion [43]. The PANI (ES) and PANI (LB) redox couple has been regarded as being responsible for establishing the potential of iron in passive region [44,45] and the PANI (LB) which has been reduced is cyclically oxidized to PANI (ES) by the reduction of oxygen so that the potential of iron is maintained always in the noble values [46,26].

The oxide film is reported to be γ-Fe_2O_3 [16] along with iron–dopant salt film [9]. Hence, the higher corrosion protection offered by PANI–Fe_2O_3 composite with phosphate dopant containing coating may be due to the formation of passive film along with iron–phosphate salt film on the iron surface. But in the case of bare Fe_2O_3 containing coating, the corrosion protection is mainly due to the barrier effect which offers less amount of corrosion protection in comparison to that of PANI–Fe_2O_3 composite containing coating.

4. Conclusions

The polyaniline–Fe_2O_3 composite has been prepared by chemical oxidative method in the presence of aniline and Fe_2O_3 by ammonium persulphate oxidant in phosphoric acid medium.

The XRD pattern shows that the polyaniline has no effect on the crystalline behaviour of Fe_2O_3. The corrosion resistant property of the coating containing 1:1 composite is found to be higher than that of Fe_2O_3 and other 1:2 and 2:1 polyaniline–Fe_2O_3 composites.

Acknowledgement

References

[1] P.J. Kinlen, D.C. Silverman, C.R. Jeffreys, Synth. Met. 85 (1997) 1327.
[2] W.K. Lu, R.L. Elsenbaumer, B. Wessling, Synth. Met. 71 (1995) 2163.
[3] B. Wessling, J. Posdorfer, Electrochim. Acta 44 (1999) 2139.
[4] D.E. Tallmen, Y. Pae, G.P. Bierwagen, Corrosion 55 (1999) 779.
[5] A. Talo, P. Passiniemi, O. Forsen, S. Ylasaari, Synth. Met. 85 (1997) 1333.
[6] S.P. Sitaram, J.O. Stoffer, T.J. O' Keefe, J. Coat. Technol. 69 (1997) 65.
[7] J.R. Santros Jr., L.H.C. Mattoso, A.J. Mothed, Electrochim. Acta 43 (1998) 309.
[8] W.S. Araujo, I.C.P. Margarit, M. Ferreiva, O.R. Mattos, P. Lima Neto, Electrochim. Acta 46 (2001) 1307.
[9] P.J. Kinlen, V. Menon, Y. Ding, J. Electrochem. Soc. 146 (1999) 3690.
[10] A.B. Samui, A.S. Patenkar, J. Rengarajan, P.C. Deb, Prog. Org. Coat. 47 (2003) 1.
[11] S. Sathiyanarayanan, S. Muthukrishnan, G. Venkatachari, D.C. Trivedi, Prog. Org. Coat. 53 (2005) 297.
[12] P.J. Kinlen, J. Ding, D.C. Silverman, Corrosion 58 (2002) 490.
[13] A.B. Samui, S.M. Phadnis, Prog. Org. Coat. 54 (2005) 263.
[14] S. Sathiyanarayanan, S. Muthukrishnan, G. Venkatachari, Prog. Org. Coat. 54 (2006) 5.
[15] S. de Souza, J.E.P. da Silva, S.I.C. de Torresi, M.L.A. Temperini, P.M. Torresi, Electrochem. Solid State Lett. 4 (2001) B27.
[16] B. Wessling, Synth. Met. 5 (1997) 1313.
[17] S. de Souza, J.E.P. da Silva, S.I.C. de Torros, M.L.A. Temperani, R.M. Torresi, Electrochem. Solid State Lett. 4 (2001) B27.
[18] A.J. Dominis, G.M. Spinks, G.G. Wallace, Prog. Org. Coat. 48 (2003) 43.
[19] W. Lu, R.L. Eisenbaumer, B. Wessling, Synth. Met. 71 (1995) 2163.
[20] N. Plesu, G. Ilia, A. Pascariu, G. Vlase, Synth. Met. 156 (2006) 230.
[21] B. Wessling, Adv. Mater. 6 (1994) 226.
[22] M. Fahlman, S. Jastr, A.J. Epstein, Synth. Met. 85 (1997) 1323.
[23] S. Syed Azim, S. Sathiyanarayanan, G. Venkatachari, Prog. Org. Coat. 56 (2006) 154.
[24] S. Sathiyanarayanan, S. Muthukrishnan, G. Venkatachari, Electrochim. Acta 51 (2006) 6313.
[25] S. Sathiyanarayanan, S. Muthukrishnan, G. Venkatachari, J. Appl. Polym. Sci. 102 (2006) 3994.
[26] R.J. Holness, G. Williams, D.A. Worsely, H.N. McMurray, J. Electrochem. Soc. 152 (2005) B73.
[27] M. Kryszawski, J.K. Jezka, Synth. Met. 94 (1998) 99.
[28] Q.l. Yang, J. Zhai, L. Feng, Y.L. Song, M.X. Wan, L. Jiang, W.G. Xu, Q.S. Li, Synth. Met. 135–136 (2003) 819.
[29] H. Tamura, E. Mathijevic, L. Meites, J. Colloid Interface Sci. 92 (1983) 303.
[30] M.A. Blesa, A.J.G. Maroto, A.L. Regazoni, J. Colloid Interface Sci. 101 (1984) 410.
[31] A.H. Gemeay, J.A. Mansour, R.G.El. Sharkaway, A.B. Zaki, Eur. Polym. J. 41 (2005) 2575.
[32] S. Sathiyanarayanan, S. Syed Azim, G. Venkatachari, Electrochim. Acta 52 (2007) 2068.
[33] F. Mansfeld, Corrosion 37 (1981) 301.
[34] C.H. Hsu, F. Mansfeld, Corrosion 57 (2001) 747.
[35] X. Li, G. Wang, X. Li, D. Lu, Appl. Surf. Sci. 229 (2004) 395.
[36] C. Wang, Z. Tan, Y. Li, L. Sun, T. Zhan, Thermochim. Acta 441 (2006) 191.
[37] M. Wan, M. Li, J. Li, Z. Liu, J. Appl. Polym. Sci. 53 (1994) 131.
[38] Hl.L. Wang, L. Toppare, J.E. Fernandez, Macromolecules 23 (1990) 1053.
[39] X. Hshenag, W. Qi, Chem. Mater. 14 (2002) 2158.
[40] J. Sapurina, A. Riede, J. Stefskal, Synth. Met. 123 (2001) 5037.
[41] J. Stefskal, O. Quadrat, J. Sapurina, J. zemek, A. Drelinkiewicz, M. Harik, I. Krivka, J. Prokes, Eur. Polym. J. 38 (2002) 631.
[42] J. Stefskal, M. Trchova, J. Brodinova, P. Kalendra, S.F. Fedorora, J. Prokes, J. Zemek, J. Colloid Interface Sci. 298 (2006) 87.
[43] G.M. Spinks, A.J. Dominis, G.G. Wallace, D.E. Tallman, J. Solid State Electrochem. 6 (2002) 85.
[44] M.C. Bernadrd, J.L. Goff, C. Joiret, N.N. Ginh, N.N. Toan, J. Electrochem. Soc. 146 (1999) 995.
[45] T. Schauer, A. Joos, Z. Dulog, C.D. Einsenbech, Prog. Org. Coat. 33 (1998) 20.
[46] R. Gasprac, R.C. Martin, J. Electrochem. Soc. 148 (2001) B138.